Published in final edited form as:
Cancer Res. 2011 February 15; 71(4): 1302–1312. doi:10.1158/0008-5472.CAN-10-3317.

MTGR1 Is Required for Tumorigenesis in the Murine AOM/DSS Colitis-Associated Carcinoma Model

Caitlyn W. Barrett[2,5], **Barbara Fingleton**[2,5], **Amanda Williams**[1,2,5], **Wei Ning**[1,2,5], **Melissa A. Fischer**[3,5], **Mary K. Washington**[4], **Rupesh Chaturvedi**[1,6], **Keith T. Wilson**[1,2,5,6], **Scott W. Hiebert**[3,5], and **Christopher S. Williams**[1,2,5]

[1]Department of Medicine/Gastroenterology, Vanderbilt University School of Medicine, Nashville, Tennessee.

[2]Department of Cancer Biology, Vanderbilt University School of Medicine, Nashville, Tennessee.

[3]Department of Biochemistry, Vanderbilt University School of Medicine, Nashville, Tennessee.

[4]Department of Pathology, Vanderbilt University School of Medicine, Nashville, Tennessee.

[5]Vanderbilt Ingram Cancer Center, Vanderbilt University School of Medicine, Nashville, Tennessee.

[6]Veterans Affairs Tennessee Valley Healthcare System, Nashville, Tennessee.

Abstract

Myeloid Translocation Gene, Related-1 (MTGR1) CBFA2T2 is a member of the Myeloid Translocation Gene (MTG) family of transcriptional corepressors. The remaining two family members, MTG8 (RUNX1T1) and MTG16 (CBFA2T3) are identified as targets of chromosomal translocations in acute myeloid leukemia (AML). *Mtgr1*$^{-/-}$ mice have defects in intestinal lineage allocation and wound healing. Moreover, these mice show signs of impaired intestinal stem cell function. Based on these phenotypes, we hypothesized that MTGR1 may influence tumorigenesis arising in an inflammatory background. We report that *Mtgr1*$^{-/-}$ mice were protected from tumorigenesis when injected with azoxymethane (AOM) and then subjected to repeated cycles of dextran sodium sulfate (DSS). Tumor cell proliferation was comparable, but *Mtgr1*$^{-/-}$ tumors had significantly higher apoptosis rates. These phenotypes were dependent on epithelial injury, the resultant inflammation, or a combination of both as there was no difference in aberrant crypt foci (ACF) or tumor burden when animals were treated with AOM as the sole agent. Gene expression analysis indicated that *Mtgr1*$^{-/-}$ tumors had significant upregulation of inflammatory networks, and immunohistochemistry (IHC) for immune cell subsets revealed a marked multilineage increase in infiltrates, consisting predominately of CD3^{+} and natural killer T (NKT) cells as well as macrophages. Transplantation of wild type (WT) bone marrow into *Mtgr1*$^{-/-}$ mice, and the reciprocal transplant, did not alter the phenotype, ruling out an MTGR1 hematopoietic cell-autonomous mechanism. Our findings indicate that MTGR1 is required for efficient inflammatory carcinogenesis in this model, and implicate its dysfunction in colitis-associated carcinoma. This represents the first report functionally linking MTGR1 to intestinal tumorigenesis.

Corresponding Author: Christopher S. Williams, Assistant Professor of Medicine and Cancer Biology, Vanderbilt University School of Medicine, 1065D MRB-IV, B2215 Garland Ave Nashville, TN 37235-0654. Phone: (615) 322-3642; Fax: (615) 343-6229; christopher.williams@vanderbilt.edu.

Note: Supplementary data for this article are available at Cancer Research Online (http://cancerres.aacrjournals.org/).

Disclosure of Potential Conflicts of Interest
No potential conflicts of interest were disclosed.

Introduction

Myeloid Translocation Gene, Related-1 (MTGR1) CBFA2T2, MTG8 (RUNX1T1) and MTG16 (CBFA2T3) are members of a gene family (MTGs) in which MTG8 and MTG16 were originally identified as targets of chromosomal translocations in acute myeloid leukemia (AML; 1, 2). Translocations involved in cancer identify master regulatory genes often affecting cellular proliferation, differentiation, and apoptosis. MTGs are transcriptional corepressors lacking both enzymatic activity and DNA binding capabilities, and act as scaffolding proteins upon which other transcriptional corepressors (mSin3a, N-CoR, SMRT), histone deacetylases, and transcription factors assemble, thus directing promoter-specific targeting of repressor complexes (1, 2). The aggregate effect of these complexes is chromatin remodeling via post-translational histone modifications.

In addition to their pivotal role in AML, MTG8 and MTG16 have been implicated in epithelial malignancies, with the identification of multiple nonsynonymous mutations in MTG8 and MTG16 in colorectal carcinoma (CRC; 3, 4) and more recently additional mutations in MTG8 identified in breast and lung cancer (5). Furthermore, MTG16 is proposed to function as a tumor suppressor in breast cancer (6). Recently, it has been demonstrated that MTGs bind to transcription factor 4 (TCF4) and repress its transcriptional activity, thus linking MTGs with a stem cell regulatory pathway critical for epithelial homeostasis that is frequently targeted in malignancy (7). The role in tumorigenesis of MTGR1, the third MTG family member, has yet to be determined.

Observations made in *Mtgr1*$^{-/-}$ and *Mtg8*$^{-/-}$ mice have identified MTGs as participating in intestinal developmental and differentiation programs. Roughly a third of *Mtg8*$^{-/-}$ mice demonstrate a complete deletion of the midgut (8). *Mtg16*$^{-/-}$ mice revealed that MTG16 is required for hematopoietic progenitor cell fate decisions and early progenitor differentiation (9). *Mtgr1*$^{-/-}$ mice have increased intestinal proliferation and the progressive depletion of the secretory lineage in the small intestine, indicating that MTGR1 regulates intestinal proliferation and differentiation programs (10). Additionally, *Mtgr1*$^{-/-}$ mice are sensitive to DSS-induced colitis and exhibit chronic architectural changes with this type of injury implicating MTGR1 in epithelial repair programs (11). Collectively, the genetic evidence suggests that MTG proteins play key roles in intestinal biologic processes and could influence intestinal tumorigenesis.

Chronic inflammation, as in Ulcerative Colitis and Crohn's Colitis, predisposes to malignancy (12–14), but with an extended latency. While inflammation can be linked to tumorigenesis, the long latency makes the molecular basis of these links less clear. Moreover, in certain malignancies inflammation may impair tumor growth. This is termed "tumor immunoediting" and represents the dynamic nature between the antitumoral and protumoral activities of immunity (15). Thus it is difficult to predict the impact a particular gene or pathway may have on tumorigenesis *a priori*.

We hypothesized that MTGR1 could modify inflammatory carcinogenesis, but whether this would be stimulatory or inhibitory was unclear. In order to test this hypothesis, we applied the azoxymethane/dextran sodium sulfate (AOM/DSS) murine inflammatory colitis model to *Mtgr1*$^{-/-}$ mice. This model has been employed to dissect NF-kB (16), toll-like receptor 4 (TLR4) (17), and tumor necrosis factor (TNFα) (18) signaling, innate immune responses (19), and the role of intestinal microflora (20) in inflammatory carcinogenesis. We found a striking decrease in tumor formation in the absence of MTGR1 coupled with increased intratumoral apoptosis. This phenotype required injury and was nonhematopoietic cell autonomous; however, global gene expression analysis revealed that members of WNT networks were decreased and genes associated with innate and adaptive immune networks

upregulated in *Mtgr1*$^{-/-}$ tumors, implicating tumor immunity as a potential mechanism of tumor clearance. Supporting this concept, we observed decreased nuclear β-catenin and increased CD3^{+}, B220^{+}, NKp46^{+}, and F4/80^{+} infiltrates in *Mtgr1*$^{-/-}$ tumors. Thus, MTGR1 is required for efficient AOM/DSS-induced tumorigenesis and may promote survival of initiated colonocytes perhaps by its influence on suppressing tumor immunity.

Methods

Murine inflammatory carcinogenesis protocol

Eight- to ten-week old C57BL/6/129 mixed background wild type (WT; $n = 22$) or *Mtgr1*$^{-/-}$ ($n = 19$) mice were injected with 12.5 mg/kg of AOM (Sigma-Aldrich) intraperitoneally as described by Greten and colleagues (21). After a 3-day recovery period, the animals were started on the first of four cycles of 3% DSS *ad libitum* (See Schematic in Fig. 1A). Each cycle lasted 5 days and was separated by a 16-day recovery period. After the last cycle, animals were sacrificed following a 26-day recovery period. Tumor counts and measurements were performed in a blinded fashion under a stereo-dissecting microscope. Microscopic analysis was performed for severity of inflammation (22) and dysplasia on (H&E) stained "Swiss rolled" colons by a gastrointestinal pathologist (MKW). All *in vivo* procedures were carried out in accordance with protocols approved by the Vanderbilt Institutional Animal Care and Use Committee.

Mtgr1 expression

Tumors and adjacent nontumor tissue from four colons were dissected from WT mice and RNA was isolated using the RNEasy MiniKit (Qiagen). SYBR Green (Bio-Rad) qRT-PCR using *Mtgr1* and glyceraldehyde 3-phosphate dehydrogenase (GAPDH) specific primers was performed in triplicate as previously described (11). Analysis of fold-change was performed using the $^{\Delta\Delta}$Ct method.

In situ hybridization

The MTGR1–1699T and MTGR1–2020B probe set and protocol of Amann and colleagues were used (10). Images were taken on a Zeiss Axioskop under identical conditions.

Immunohistochemistry

Two hours prior to sacrifice, animals were injected with 16.7 mg/kg bromodeoxyuridine. Five micrometer sections were cut, dewaxed, hydrated and endogenous peroxidase activity quenched with 0.03% hydrogen peroxide in MeOH. Antigen retrieval was performed using the boiling sodium citrate method in a microwave (20 mmol sodium citrate pH 6.5) for 16 minutes at 30% power. After blocking, primary antibody was added (α-β-catenin, (BD Transduction Laboratories), 1:1000; α-CD3, (Serotec), 1:1000; α-CD45r, (BD Pharmingen), 1:40, monoclonal α-BrdU (Accurate Labs) 1:2000), α-arginase I (ARG1), (Santa Cruz), 1:500; α-IL-1β, (R&D Systems), 1:50; α-NKp46, (Santa Cruz), 1:500; α-matrilysin 338 (23), diluted 1:500) overnight at 4°C. Isotype-matched antibodies were included as negative controls. The Vectastain ABC Elite System (Vector Labs) was used to visualize staining for IHC. For immunofluorescence, slides were counterstained with DAPI (Invitrogen) and mounted with ProLong Gold antifade (Invitrogen). Identification of intratumoral apoptotic cells was performed using the ApopTag Plus Peroxidase *in situ* Apoptosis Kit (Chemicon) according to the manufacturer's protocol. Control stains were obtained by omitting the terminal transferase (TnT) enzyme. Immune cell, apoptosis, and proliferation indices were generated by counting the number of positive cells per high-powered field (HPF; 40× objective) within each tumor (15 *Mtgr1*$^{-/-}$ 42 WT tumors) from 9 *Mtgr1*$^{-/-}$ and 14 WT tumor bearing mice. A total of 82 *Mtgr1*$^{-/-}$ and 319 WT HPFs were examined and the mean

positive cells per HPF was calculated. A crypt apoptosis and proliferation index was generated by counting 20 crypts per mouse. This is presented as the mean number of $TUNEL^+$ or $BrdU^+$ cells per crypt.

Cell culture and siRNA transfection

Human colon tumor (HCT116) cells were obtained from Dr. Robert Coffey and have morphologic characteristics consistent with their known identity. Formal authentication was not performed. One day prior to siRNA transfection, cells were plated at 2×10^5 cells per well in a 6-well plate. Cells were then transfected with ON-TARGETplus SMARTpool siRNA for *Mtgr1*/CBFA2T2 (Thermo Scientific) using RNAiMax (Invitrogen) according to the manufacturer's protocol. Six hours after transfection, the transfection mixture was replaced with complete media. The next day, cells were starved overnight with media containing 1% bovine serum albumin (BSA) and the next morning cells were washed and complete media was added. After harvesting, cells were analyzed for apoptosis using the TACS Annexin V-FITC flow cytometry kit (R&D Systems). Cells were analyzed on the 5-laser BD LSRII analyzer and unstained controls were used to establish proper gating. Presented are the average percentage of annexin V positive cells per 10,000 cells over three different trials.

Expression array assays

Tumors were dissected from WT and $Mtgr1^{-/-}$ mice and RNA was isolated using the RNEasy MiniKit (Qiagen). RNA integrity was determined using an Agilent 2100 Bioanalyzer (Agilent Technologies, Santa Clara, CA). All RNA samples had RNA integrity numbers (RINs) >8 and were deemed suitable for hybridization. A total of 10 mg of cRNA was used in the second cycle of first strand synthesis to generate the correct sense for target hybridization. Mouse gene 1.0 ST arrays (Affymetrix) were scanned the next day. CEL files were imported into Partek Express (Partek) and Robust Multichip Average (RMA) was run across all eight samples. Pivot data was exported and posted. A *t*-test was run between the $Mtgr1^{-/-}$ and WT sample groups in Partek. The *P*-value was multiple testing corrected with Bonferroni and Step-up. Expression array analysis was performed hybrizing cRNA to the Mouse gene 1.0 ST chip (Affymetrix). Differentially expressed genes were classified using the PANTHER (Protein Analysis THrough Evolutionary Relationships) classification system (www.pantherdb.org/gen).

Bone marrow transplant

A single cell suspension of bone marrow cells was obtained from the tibia and femur of two $Mtgr1^{-/-}$ and four WT 6-week old donor mice, and the red blood cells were lysed with erythrocyte lysis buffer (Buffer EL, Qiagen). 0.85×10^6 bone marrow cells were injected via the tail vein into 15 $Mtgr1^{-/-}$ and 17 WT lethally irradiated (900 rads) 8–12-week old recipient mice. The mice were then fed acidified water (0.015% HCl in autoclaved water) supplemented with 1.1 g/L neomycin sulfate and 125 mg/L polymyxin B sulfate for 2 weeks post-transplantation (modified from Cotta and colleagues. (24)). Eight weeks post-transplantation, the mice were placed on the Murine Inflammatory Carcinogenesis Protocol.

Statistical methods

Apoptosis, proliferation, and immune cell indices as well as the tumor and burden counts were analyzed using the Student's *t*-test using Graphpad Prism 5.0c, unless otherwise indicated.

Results

Mtgr1 is overexpressed in AOM/DSS tumors

Proteins regulating intestinal proliferation and differentiation pathways often contribute to oncogenesis. Given the newly discovered role of MTGR1 in regulating these processes coupled with the observation that loss of MTGR1 results in sensitization to gut injury, we hypothesized that *Mtgr1* expression may be altered in AOM/DSS tumors. For these experiments, 8–10-week-old mice were injected with AOM and treated with four cycles of DSS as defined in the Methods section and shown in Figure 1A. Tumors and adjacent tissue were harvested and both qRT-PCR and *in situ* hybridization for *Mtgr1* mRNA expression was performed. A 10.7-fold increase ($P < 0.001$) in *Mtgr1* mRNA expression was demonstrated in tumors compared to adjacent mucosa (Fig. 1B) and this expression was localized to a majority of the epithelial cells within the tumor whereas in adjacent histologically normal appearing colonic crypts it was expressed in only a small population of epithelial cells within the lower crypt region, consistent with the published expression pattern (Fig. 1C; 10). We next wanted to determine if *MTGR1* levels varied in human colon cancer. We were unable to obtain human colitis associated carcinoma samples therefore we performed qRT-PCR for *MTGR1* on two colorectal cancer sample groups. The first consisted of nonmatched normal and CRC tissues. In this group, we observed a 2.3-fold increase in *MTGR1* expression in the CRC samples ($P < 0.05$; Supplementary Fig. S1A). We then looked at nine matched normal/colon cancer samples and found heterogeneity in MTGR1 expression, however, 55% of the CRC samples demonstrated an increase in *MTGR1* expression (Supplementary Fig. S1B). These results suggest that MTGR1 may contribute to inflammatory carcinogenesis in the colon and we postulated that deletion of MTGR1 may prevent tumor formation.

Mtgr1 is required for efficient inflammatory tumorigenesis

Using genetic manipulation in the mouse, we tested whether MTGR1 was required for tumorigenesis in the AOM/DSS model. Eight- to ten-week-old WT or $Mtgr1^{-/-}$ mice were placed on the AOM/DSS protocol (Fig. 1A). Consistent with our prior report (11) $Mtgr1^{-/-}$ mice experienced greater weight loss in comparison to WT animals with each DSS treatment. Looser stool was evident in both groups, with frank blood frequently seen in the $Mtgr1^{-/-}$ mice. Four weeks after the last DSS cycle, the animals were sacrificed. Despite the increased sensitivity to colitis, the $Mtgr1^{-/-}$ mice actually had significantly fewer polyps compared to WT mice (1.8 ± 0.5 vs 7.5 ± 0.8, Fig. 2A) and decreased tumor size (4.6 ± 0.62 mm^2 vs 8.4 ± 0.83 mm^2, Fig. 2B), which was apparent upon gross inspection (representative colons, Fig. 2C). Histologic examination of H&E stained sections from colons prepared as "Swiss Rolls" revealed adenomas with high grade dysplasia characterized by loss of epithelial polarity and a more complex tumor growth pattern frequently present in WT tumors, whereas the adenomas observed in the $Mtgr1^{-/-}$ colons (Fig. 2D) more often showed only low grade dysplastic changes. WT or $Mtgr1^{-/-}$ mice treated either with AOM as a single modality, or with multiple exposures to DSS in the absence of AOM, did not develop tumors over this time frame (data not shown).

A decrease in tumor multiplicity in $Mtgr1^{-/-}$ mice suggested that MTGR1 may be playing a role in initiated or early tumor progenitor cell survival after injury, as opposed to influencing tumor promotion, in which case similar number of tumors, but smaller tumors would be expected. To determine if epithelial injury was required for this effect, we treated animals with AOM as a single agent (12.5 mg/kg IP) and assessed effects 48 weeks later. At necropsy, there was no difference in polyp or aberrant crypt foci (ACF) formation between WT and $Mtgr1^{-/-}$ mice (polyps, 3.5 ± 0.2 vs 4.1 ± 0.5, $P = 0.40$; ACF, 23.4 ± 0.1 vs 27.0 ±2.0, $P = 0.21$, Supplementary Fig. S2A, B). These data indicate that alterations in epithelial

injury, either due to DSS itself or due to inflammatory infiltration was required for the different AOM/DSS phenotype in *Mtgr1*$^{-/-}$ versus WT mice. Collectively, these experiments suggest that MTGR1 could protect early tumor progenitor cells from clearance after enterocyte injury.

Altered intratumoral apoptosis in the absence of MTGR1

Variations in proliferation or apoptosis may account for the difference in tumor burden between *Mtgr1*$^{-/-}$ and WT mice. Intratumoral apoptosis rates were assessed using *in situ* terminal deoxynucleotidyl transferase dUTP nick end labeling (TUNEL) staining. *Mtgr1*$^{-/-}$ mice demonstrated an average of 32.0 ± 5.1 TUNEL^{+} cells/tumor HPF. WT mice, on the other hand, displayed 12.9 ± 0.9 TUNEL^{+} cells/tumor HPF ($P < 0.001$, Fig. 3A), while no differences were seen in apoptotic indices within crypts. To investigate whether there is a direct link between loss of MTGR1 and induction of apoptosis, we utilized a cell culture model using the human colon cancer cell line HCT116. Knockdown of MTGR1 by siRNA resulted in increased apoptosis as measured by annexin V and propidium iodide (PI) flow cytometry (Fig. 3B), but no change in proliferation (data not shown).

Next, to analyze proliferation rates, BrdU immunohistochemistry (IHC) was performed. BrdU positive cells/crypt were counted and averaged. As observed previously (11), nontumorigenic *Mtgr1*$^{-/-}$ colonic epithelium showed a modest increase in proliferation compared to WT mice (5.2 ± 0.3 vs 4.3 ± 0.2 BrdU positive cells/crypt, $P = 0.02$, Supplementary Fig. 3A). However, intratumoral proliferation rates were similar between WT and *Mtgr1*$^{-/-}$ mice (100.2 ± 12.3/HPF vs 82.7 ± 7.3/HPF, $P = 0.28$, Supplementary Fig. 3A), suggesting that the difference in tumor formation and/or size was not a function of differences in epithelial proliferation rates between WT and *Mtgr1*$^{-/-}$ animals, but more likely due to differences in intratumoral apoptosis.

Decreased nuclear and total β-catenin in *Mtgr1*$^{-/-}$ tumors

All three MTG family members (MTGR1, MTG16, and MTG8) are capable of competing with β-catenin for TCF4 occupancy and can repress TCF4 mediated transcriptional activity (7). Based on this observation, we stained WT or *Mtgr1*$^{-/-}$ tumors with a β-catenin specific antibody to determine the levels of β-catenin expression and its localization. We derived a β-catenin staining index, which incorporates the intensity of staining and percentage of nuclear β-catenin^{+} cells/HPF. We found uniformly high nuclear and cytoplasmic staining in the WT tumors (252.4 ±24.9, Fig. 4A and B). However, the *Mtgr1*$^{-/-}$ tumors contained lower levels of nuclear β-catenin and there was a more heterogeneous staining pattern within the tumor (101.2 ± 23.6, Fig. 4A and B).

Transcriptional network alterations in *Mtgr1*$^{-/-}$ tumors

To address the mechanism by which MTGR1 might act during tumorigenesis, RNA was isolated from WT and *Mtgr1*$^{-/-}$ tumors and hybridized to Affymetrix Mouse Gene 1.0 ST arrays. After data normalization, expression profiles were uploaded to the PANTHER platform (25). Significant decreases in both Wnt ($P = 0.001$) and Cadherin ($P = 0.0001$) pathways in the *Mtgr1*$^{-/-}$ tumors were evident with the most significant reductions in the WNT target *Lgr5* (−8.95-fold), consistent with decreased WNT signaling tone in the *Mtgr1*$^{-/-}$ tumors. Paradoxically, repressors of WNT signaling (*Wif1* −17.9x, *Dkk2* −7.6x, and *Axin2* −3.8x, Supplemental Table 1) were also downregulated. Levels of expression of the matrix metalloproteinases (*Mmp-7* 6.8x, *Mmp-13* 3.9x, *Mmp-12* 3.5x, and *Mmp-14* 3.4x) were also decreased in *Mtgr1*$^{-/-}$ tumors (Supplemental Table 1). MMP7 is a known target gene of the WNT pathway (26) and its overexpression has been associated with colon cancer (27). We therefore assessed MMP7 at the protein level by immunofluorescence, and observed not only decreased expression but also decreased secretion of MMP7 from colonic

polyps in the *Mtgr1*$^{-/-}$ versus WT mice (Fig. 5A and B). These findings suggest that decreases in WNT signaling and MMP expression may contribute to decreased tumor size in *Mtgr1*$^{-/-}$ mice.

Immune pathways are upregulated in *Mtgr1*$^{-/-}$ tumors

PANTHER analysis of the changes in gene expression also revealed increased MHC-I (P = 0.001), MHC-II (P = 0.003), T-cell ($P = 6.8 \times 10^{-11}$), and B-cell mediated immunity pathways (P = 0.007), indicating that these gene classes are over-represented in the *Mtgr1*$^{-/-}$ tumors (Supplementary Table 2). To both confirm and extend these observations, we performed immunohistochemistry on WT and *Mtgr1*$^{-/-}$ tumors to classify intratumoral inflammation. In *Mtgr1*$^{-/-}$ vs WT tumors (Fig. 6A and B), there were increased CD3^{+} T-lymphocytes (13.6 ± 2.5/tumor HPF vs 49.4 ± 5.6, $P < 0.001$), B220/CD45r^{+} B-lymphocytes (15.8 ± 2.3 vs 6.0 ± 0.8/tumor HPF, $P < 0.001$), and NKp46^{+} natural killer cells (51.0 ± 3.7 vs 36.0 ± 3.1/tumor HPF, P = 0.004). Because *Mtgr1*$^{-/-}$ tumors were smaller than WT tumors and mononuclear phagocytes can exert antitumor activity by directly killing tumor cells and eliciting tissue disruptive reactions (28), we used F4/80 and IL-1β costaining and observed increased M1 macrophages in *Mtgr1*$^{-/-}$ tumors (29.1 ± 3.0 positive cells/tumor HPF vs 11.6 ± 1.6, $P < 0.001$). Because M2 macrophages are generally considered protumorigenic (28), we anticipated that costaining with F4/80 and ARG1 would identify fewer M2 mononuclear cells in the *Mtgr1*$^{-/-}$ tumors. We were surprised to find increased M2 cells in the *Mtgr1*$^{-/-}$ tumors (15.8 ± 2.6 positive cells/tumor HPF vs 7.2 ± 1.3, P = 0.003, Fig. 6A and B).

In situ hybridization indicated that *Mtgr1* was mainly expressed within the epithelium of developing AOM/DSS induced tumors (Fig. 1C). However, MTGR1 is present in many tissue types, including hematopoietic lineages (29). Given the dramatic changes in inflammatory cell infiltration in the tumors, MTGR1 could be acting in a hematopoietic cell autonomous fashion to repress immune infiltration, or alternatively, MTGR1 could be acting in the stromal or epithelial compartment to repress immune cell recruitment. To test whether the MTGR1 effect is hematopoietic cell autonomous, we restored MTGR1 expression in hematopoietic cells in the *Mtgr1*$^{-/-}$ mouse via bone marrow transplantation of WT marrow. In addition, WT mice were transplanted with *Mtgr1*$^{-/-}$ marrow and control transplants consisting of WT or *Mtgr1*$^{-/-}$ mice transplanted with WT or *Mtgr1*$^{-/-}$ marrow, respectively, were also performed (Fig. 7A and B). Nontransplanted controls did not survive 2 weeks post-irradiation, indicating that the endogenous marrow was ablated. Transplanted animals were allowed to recover for 3 months prior to placing the animals on the AOM/DSS protocol.

WT mice rescued with either WT or *Mtgr1*$^{-/-}$ bone marrow had equivalent tumor burden (2.125 ± 0.693 and 1.5 ± 0.756, polyps/mouse, respectively). No tumors were observed in either of the *Mtgr1*$^{-/-}$ recipient groups. This indicates, at least in this model, that it is the absence of MTGR1 in nonhematopoietic cellular compartments that protects from AOM/DSS-induced tumorigenesis. This data coupled with increased epithelial apoptosis in the HCT-116 cells suggests that MTGR1 promotes tumorigenesis through its actions in the epithelium.

Discussion

Myeloid Translocation Genes (MTGs) are transcriptional corepressors that were first identified in AML where the prototypic event is the 8:21 translocation (30). Considerable information has been gained from the creation of constitutional null alleles for each MTG family member. *Mtgr1*$^{-/-}$ mice have increased enterocyte proliferation, mainly localized to the lower 1/3 of the crypt, as well as the progressive depletion of the secretory lineage in the

small intestine (10). The presence of MTGR1 is required for maintenance of epithelial integrity after DSS-mediated injury and chronic architectural changes occur after a solitary DSS-mediated injury (11).

In this report, we demonstrate that MTGR1 is required for efficient inflammatory-associated colonic carcinogenesis. AOM is a procarcinogen and is metabolically activated to a potent alkylating agent forming O^6-methyl-guanine (31). Its oncogenic potential is markedly augmented in the setting of chronic inflammation, such as that induced by repeated cycles of DSS treatment (32). The power of this model has recently been demonstrated in deciphering the epithelial versus myeloid cell contribution of IKKβ to polyp formation in the setting of inflammation (21), and the contributions of IL-6 and its downstream mediator, STAT-3 (33). IL-6 and MTGR1 are required for maintenance of mucosal integrity after injury (11), (33). Both *Mtgr1*$^{-/-}$ and *IL-6*$^{-/-}$ mice are protected from tumorigenesis in the AOM/DSS model. In the case of the *Mtgr1*$^{-/-}$ mice, higher levels of intratumoral apoptosis, with no appreciable difference in proliferation, may mediate the beneficial affect of MTGR1 deletion. Injury is required for the *Mtgr1*$^{-/-}$ protective effect, as there was no difference in tumor burden when mice were injected with AOM without subsequent cycles of DSS. This suggests that MTGR1, similar to IL-6, protects initiated epithelial cells from apoptosis. In the case of IL-6, this is mediated via its production by lamina propria myeloid cells, and our data indicate that hematopoetic MTGR1 production does not modify tumorigenesis.

Alteration in WNT signaling is a common initiating event in sporadic CRC (34); however, it is less common in colitis-associated carcinoma (CAC), and when it does occur, it typically does so as a late event (35). We were surprised to find evidence of low WNT signaling in *Mtgr1*$^{-/-}$ tumors as it has previously been shown that MTGs bind to TCF4 and compete with β-catenin for occupancy; thus, at least in certain circumstances, antagonizing WNT transduced signals (7). One potential explanation for this apparent paradox is that MTGs are known to function as transcriptional corepressors via diverse interactions with multiple transcription factors (i.e., PLZF, BCL6, GFI-1) in addition to TCF4. They also form bridging interactions with other transcriptional corepressors such as N-CoR, SMRT, mSin3A, and HDACs 1, 2, and 3 (2, 36, 37). Our results suggest that the effect of MTGR1 on WNT signaling may be less important than its ability to inhibit apoptosis via modulating other pathways.

Our data suggest that loss of MTGR1 shifts the inflammatory response towards an antitumorigenic state by increasing expression of tumoricidal immune cells such as natural killer cells and M1 macrophage subsets. Perplexingly, there is also a concomitant increase in "protumorigenic" M2 polarized macrophages. It is theorized that there is a balance between M1 (antitumorigenic) and M2 (protumorigenic) within the tumor microenvironment and it is proposed that this balance could have different net effects at different stages of tumor progression (28). As the overall observed effect in the absence of MTGR1 was smaller and fewer tumors, this observation suggests that MTGR1 could influence the balance between anti- and pro-tumorigenic macrophage function. Furthermore, the fact that WT marrow transplanted into *Mtgr1*$^{-/-}$ mice failed to prevent the reduction in tumorigenesis in the *Mtgr1*$^{-/-}$, AOM/DSS phenotype indicates that this process is not acting in an autonomous manner in hematopoietic cell in this tumor model. This raises the possibility that MTGR1 suppresses inflammatory recruitment, perhaps via regulating production of epithelial derived chemokines and cytokines.

We observed decreased *Mmp-7* (Matrilysin), *−12*, *−13*, and *−14* in *Mtgr1*$^{-/-}$ tumors. These matrix metalloproteinases are overexpressed in human CRCs with increased *Mmp-7* observed early in malignant progression and in 85% of surveyed tumors (38). *Mmp-7*$^{-/-}$ mice bred with *Apc*$^{Min/+}$ mice have a 50% decrease in polyposis (27, 39). MMP-7 has

pleiotropic effects promoting cancer progression via its proteolytic activity against the ectodomain of a number of cell surface proteins. For example, MMP-7 cleavage of CD95L makes tumor cells resistant to apoptosis (40, 41), MMP-7 mediated cleavage of proHB-EGF into mature HB-EGF promotes proliferation and angiogenesis (42), and E-cadherin is cleaved to soluble E-cadherin, promoting invasion (43). The tumor promoting effects of increased MMP expression could contribute to tumor growth differences and raises the intriguing possibility that MMPs may be important targets of MTGR1-mediated repression.

In conclusion, we demonstrate that removal of MTGR1 enhances inflammation, increases intratumoral apoptosis, and reduces production of proteins such as MMPs known to be pivotal to tumor growth. Thus, MTGR1 appears to influence the tumor microenvironment and in addition to its effects on initiated cell survival may also suppress tumor immunosurvelliance. These studies provide insight into disease pathogenesis and implicate MTGR1 dysfunction in colitis-associated carcinoma and sporadic CRC, thus providing the substrate for translational investigations of MTGR1 in colitis-associated carcinoma.

Supplementary Material

Refer to Web version on PubMed Central for supplementary material.

Acknowledgments

We thank Drs. Richard Peek, Robert Coffey, Baolin Zhang, and other members of the Williams Laboratory for thoughtful discussions regarding this research project. We also thank Frank Revetta for histologic support.

Grant Support

NIH Grant K08 DK080221–01 (C.S. Williams), CA64140 (S.W. Hiebert), CA112005 (S.W. Hiebert) and HL088494 (S. W. Hiebert), NIH P50CA095103 (M.K. Washington), AT004821 (K.T. Wilson), DK053620 (K.T. Wilson), AT004821-S1 (K.T.Wilson), a Merit Review Grant (K.T. Wilson), P30DK058404 (Pilot Project, C.S. Williams), ACS-RSG 116552 (C.S. Williams), CCFA1709 (C.S. Williams).

References

1. Davis JN, McGhee L, Meyers S. The ETO (MTG8) gene family. Gene. 2003; 303:1–10. [PubMed: 12559562]
2. Lutterbach B, Westendorf JJ, Linggi B, Patten A, Moniwa M, Davie JR, et al. ETO, a target of t(8;21) in acute leukemia, interacts with the N-CoR and mSin3 corepressors. Mol Cell Biol. 1998; 18:7176–7184. [PubMed: 9819404]
3. Sjoblom T, Jones S, Wood LD, Parsons DW, Lin J, Barber TD, et al. The consensus coding sequences of human breast and colorectal cancers. Science. 2006; 314:268–274. [PubMed: 16959974]
4. Wood LD, Parsons DW, Jones S, et al. The genomic landscapes of human breast and colorectal cancers. Science. 2007; 318:1108–1113. [PubMed: 17932254]
5. Kan Z, Jaiswal BS, Stinson J, et al. Diverse somatic mutation patterns and pathway alterations in human cancers. Nature. 466:869–873. [PubMed: 20668451]
6. Kochetkova M, McKenzie OL, Bais AJ, et al. CBFA2T3 (MTG16) is a putative breast tumor suppressor gene from the breast cancer loss of heterozygosity region at 16q24.3. Cancer Res. 2002; 62:4599–4604. [PubMed: 12183414]
7. Moore AC, Amann JM, Williams CS, Tahinci E, Farmer TE, Martinez JA, et al. Myeloid translocation gene family members associate with T-cell factors (TCFs) and influence TCF-dependent transcription. Mol Cell Biol. 2008; 28:977–987. [PubMed: 18039847]
8. Calabi F, Pannell R, Pavloska G. Gene targeting reveals a crucial role for MTG8 in the gut. Mol Cell Biol. 2001; 21:5658–5666. [PubMed: 11463846]

9. Chyla B, Moreno-Miralles I, Steapleton M, Thompson MA, Bhaskara S, Engel M, et al. Deletion of Mtg16, a target of the t(16;21), alters hematopoietic progenitor cell proliferation and lineage allocation. Mol Cell Biol. 2008; 28:6234–6247. [PubMed: 18710942]
10. Amann JM, Chyla BJ, Ellis TC, Martinez A, Moore AC, Franklin JL, et al. Mtgr1 is a transcriptional corepressor that is required for maintenance of the secretory cell lineage in the small intestine. Mol Cell Biol. 2005; 25:9576–9585. [PubMed: 16227606]
11. Martinez JA, Williams CS, Amann JM, et al. Deletion of Mtgr1 sensitizes the colonic epithelium to dextran sodium sulfate-induced colitis. Gastroenterology. 2006; 131:579–588. [PubMed: 16890610]
12. Itzkowitz SH, Yio X. Inflammation and cancer IV. Colorectal cancer in inflammatory bowel disease: the role of inflammation. Am J Physiol Gastrointest Liver Physiol. 2004; 287:G7–G17. [PubMed: 15194558]
13. Ostrand-Rosenberg S, Sinha P. Myeloid-derived suppressor cells: linking inflammation and cancer. J Immunol. 2009; 182:4499–4506. [PubMed: 19342621]
14. Berasain C, Castillo J, Perugorria MJ, Latasa MU, Prieto J, Avila MA. Inflammation and liver cancer: new molecular links. Ann N Y Acad Sci. 2009; 1155:206–221. [PubMed: 19250206]
15. Swann JB, Smyth MJ. Immune surveillance of tumors. J Clin Invest. 2007; 117:1137–1146. [PubMed: 17476343]
16. Greten FR, Eckmann L, Greten TF, Park JM, Li ZW, Egan LJ, et al. IKKbeta links inflammation and tumorigenesis in a mouse model of colitis-associated cancer. Cell. 2004; 118:285–296. [PubMed: 15294155]
17. Fukata M, Chen A, Vamadevan AS, Cohen J, Breglio K, Krishnareddy S, et al. Toll-like receptor-4 promotes the development of colitis-associated colorectal tumors. Gastroenterology. 2007; 133:1869–1881. [PubMed: 18054559]
18. Popivanova B, Kitamura K, Wu Y, Kondo T, Kagaya T, Kaneko S, et al. Blocking TNF-alpha in mice reduces colorectal carcinogenesis associated with chronic colitis. J Clin Invest. 2008; 118:560–570. [PubMed: 18219394]
19. Grivennikov S, Karin E, Terzic J, Mucida D, Yu GY, Vallabhapurapu S, et al. IL-6 and Stat3 are required for survival of intestinal epithelial cells and development of colitis-associated cancer. Cancer Cells. 2009; 15:103–113.
20. Uronis JM, Müuhlbauer M, Herfarth HH, Rubinas TC, Jones GS, Jobin C. Modulation of the intestinal microbiota alters colitis-associated colorectal cancer susceptibility. PLoS One. 2009; 4:e6026. [PubMed: 19551144]
21. Greten FR, Eckmann L, Greten TF, Park JM, Li ZW, Egan LJ, et al. IKKbeta links inflammation and tumorigenesis in a mouse model of colitis-associated cancer. Cell. 2004; 118:285–296. [PubMed: 15294155]
22. Dieleman LA, Palmen MJ, Akol H, Bloemena E, Pena AS, Meuwissen SG, et al. Chronic experimental colitis induced by dextran sulphate sodium (DSS) is characterized by Th1 and Th2 cytokines. Clin Exp Immunol. 1998; 114:385–391. [PubMed: 9844047]
23. Fingleton B, Powell WC, Crawford HC, Couchman JR, Matrisian LM. A rat monoclonal antibody that recognizes pro- and active MMP-7 indicates polarized expression in vivo. Hybridoma (Larchmt). 2007; 26:22–27. [PubMed: 17316082]
24. Cotta CV, Zhang Z, Kim HG, Klug CA. Pax5 determines B- versus T-cell fate and does not block early myeloid-lineage development. Blood. 2003; 101:4342–4346. [PubMed: 12560221]
25. Thomas PD, Campbell MJ, Kejariwal A, Mi H, Karlak B, Daverman R, et al. PANTHER: a library of protein families and subfamilies indexed by function. Genome Res. 2003; 13:2129–2141. [PubMed: 12952881]
26. Crawford HC, Fingleton BM, Rudolph-Owen LA, Goss KJ, Rubinfeld B, Polakis P, et al. The metalloproteinase matrilysin is a target of beta-catenin transactivation in intestinal tumors. Oncogene. 1999; 18:2883–2891. [PubMed: 10362259]
27. Wilson CL, Heppner KJ, Labosky PA, Hogan BL, Matrisian LM. Intestinal tumorigenesis is suppressed in mice lacking the metalloproteinase matrilysin. Proc Natl Acad Sci U S A. 1997; 94:1402–1407. [PubMed: 9037065]

28. Allavena P, Sica A, Garlanda C, Mantovani A. The Yin-Yang of tumor-associated macrophages in neoplastic progression and immune surveillance. Immunol Rev. 2008; 222:155–161. [PubMed: 18364000]
29. Morohoshi F, Mitani S, Mitsuhashi N, Kitabayashi I, Takahashi E, Suzuki M, et al. Structure and expression pattern of a human MTG8/ETO family gene, MTGR1. Gene. 2000; 241:287–295. [PubMed: 10675041]
30. Kozu T, Komori A, Sueoka E, Fujiki H, Kaneko Y, Matsui T, et al. Significance of MTG8 in leukemogenesis. Leukemia. 1997; 11 Suppl 3:297–298. [PubMed: 9209371]
31. Pegg AE. Methylation of the O6 position of guanine in DNA is the most likely initiating event in carcinogenesis by methylating agents. Cancer Invest. 1984; 2:223–231. [PubMed: 6733565]
32. Okayasu I, Ohkusa T, Kajiura K, Kanno J, Sakamoto S. Promotion of colorectal neoplasia in experimental murine ulcerative colitis. Gut. 1996; 39:87–92. [PubMed: 8881816]
33. Grivennikov S, Karin E, Terzic J, Mucida D, Yu GY, Vallabhapurapu S, et al. IL-6 and Stat3 are required for survival of intestinal epithelial cells and development of colitis-associated cancer. Cancer Cells. 2009; 15:103–113.
34. Grady WM, Carethers JM. Genomic and epigenetic instability in colorectal cancer pathogenesis. Gastroenterology. 2008; 135:1079–1099. [PubMed: 18773902]
35. Feagins LA, Souza RF, Spechler SJ. Carcinogenesis in IBD: potential targets for the prevention of colorectal cancer. Nat Rev Gastroenterol Hepatol. 2009; 6:297–305. [PubMed: 19404270]
36. Amann JM, Nip J, Strom DK, Lutterbach B, Harada H, Lenny N, et al. ETO, a target of t(8;21) in acute leukemia, makes distinct contacts with multiple histone deacetylases and binds mSin3A through its oligomerization domain. Mol Cell Biol. 2001; 21:6470–6483. [PubMed: 11533236]
37. Wang J, Hoshino T, Redner RL, Kajigaya S, Liu JM. ETO, fusion partner in t(8;21) acute myeloid leukemia, represses transcription by interaction with the human N-CoR/mSin3/HDAC1 complex. Proc Natl Acad Sci U S A. 1998; 95:10860–10865. [PubMed: 9724795]
38. Wagenaar-Miller RA, Gorden L, Matrisian LM. Matrix metalloproteinases in colorectal cancer: is it worth talking about? Cancer Metastasis Rev. 2004; 23:119–135. [PubMed: 15000153]
39. Sinnamon MJ, Carter KJ, Fingleton B, Matrisian LM. Matrix metalloproteinase-9 contributes to intestinal tumourigenesis in the adenomatous polyposis coli multiple intestinal neoplasia mouse. Int J Exp Pathol. 2008; 89:466–475. [PubMed: 19134056]
40. Fingleton B, Vargo-Gogola T, Crawford HC, Matrisian LM. Matrilysin [MMP-7] expression selects for cells with reduced sensitivity to apoptosis. Neoplasia. 2001; 3:459–468. [PubMed: 11774028]
41. Powell WC, Fingleton B, Wilson CL, Boothby M, Matrisian LM. The metalloproteinase matrilysin proteolytically generates active soluble Fas ligand and potentiates epithelial cell apoptosis. Curr Biol. 1999; 9:1441–1447. [PubMed: 10607586]
42. Yu WH, Woessner JF Jr. McNeish JD, Stamenkovic I. CD44 anchors the assembly of matrilysin/MMP-7 with heparin-binding epidermal growth factor precursor and ErbB4 and regulates female reproductive organ remodeling. Genes Dev. 2002; 16:307–323. [PubMed: 11825873]
43. Noe V, Fingleton B, Jacobs K, et al. Release of an invasion promoter E-cadherin fragment by matrilysin and stromelysin-1. J Cell Sci. 2001; 114:111–118. [PubMed: 11112695]

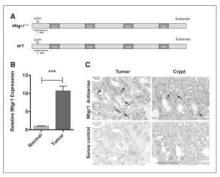

Figure 1.

Mtgr1 expression is increased in tumors resulting from AOM/DSS colitis-associated carcinoma. A, schematic of the AOM/DSS protocol. B, polyps and adjacent normal tissue subjected to Taqman qRT-PCR analysis via the delta–delta C^T method that demonstrated a 10.73-fold increase in *Mtgr1* expression in tumor versus normal tissue (***$P < 0.001$). Error bar represents the standard error for four biological replicates performed in triplicate. C, *Mtgr1 in situ* hybridization of colonic "Swiss Rolls" obtained from WT AOM/DSS. Arrows indicate positive signal within the base of the crypt. Scale bar is 5 μm.

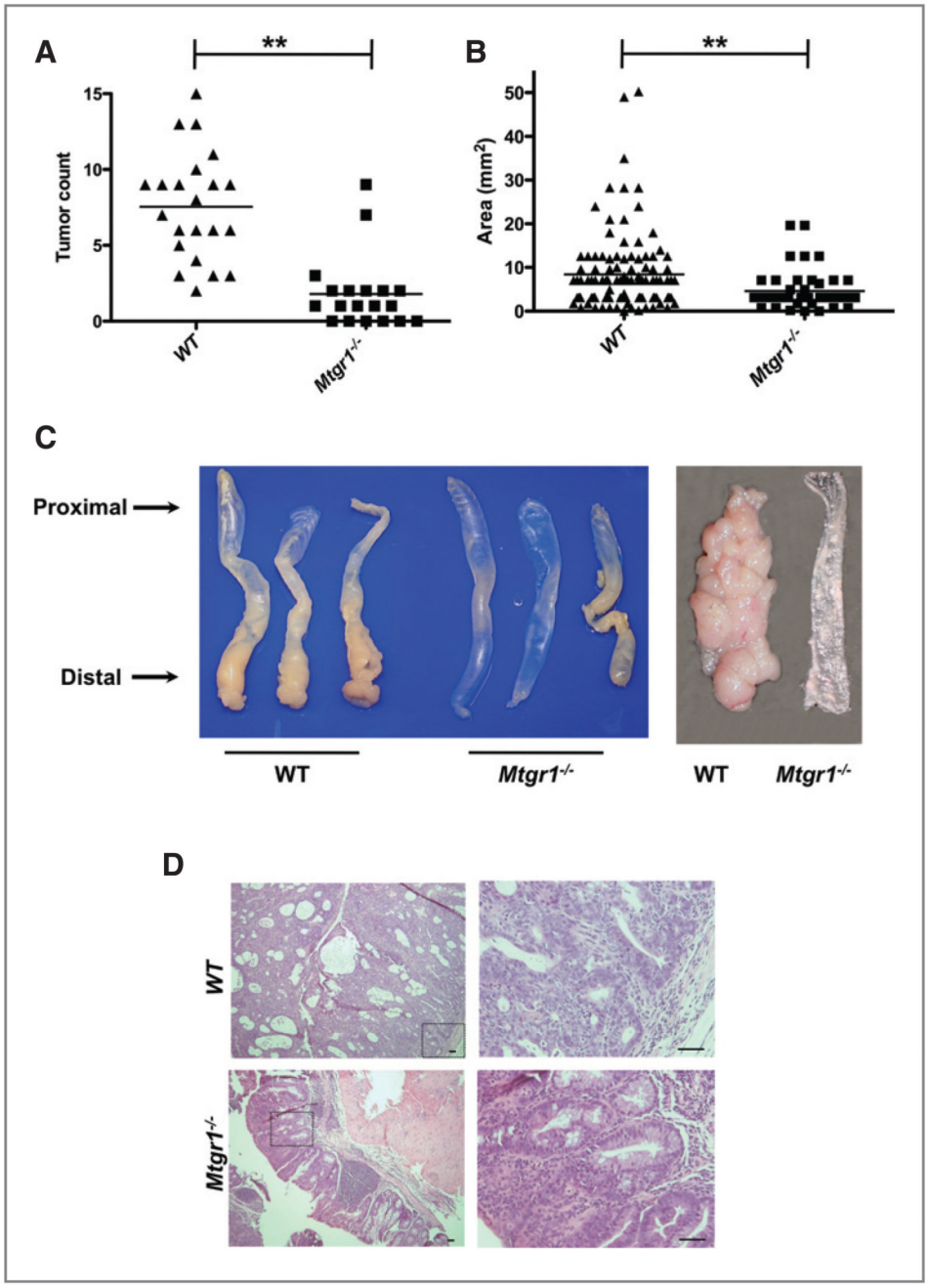

Figure 2.

MTGR1 functions as a tumor promoter in the murine AOM/DSS inflammatory carcinogenesis model. A, polyp frequency and B, polyp size as determined via calculation of the surface area of each lesion in each mouse (**$P < 0.01$).

C, representative gross specimens from three WT and *Mtgr1*$^{-/-}$ AOM/DSS treated mice with longitudinally opened colons on the far right. D, representative H&E demonstrating tumors from WT and *Mtgr1*$^{-/-}$ mice. Overall, WT tumors were larger and displayed more dysplasia than those from *Mtgr1*$^{-/-}$ mice. Scale bar is 5 μm.

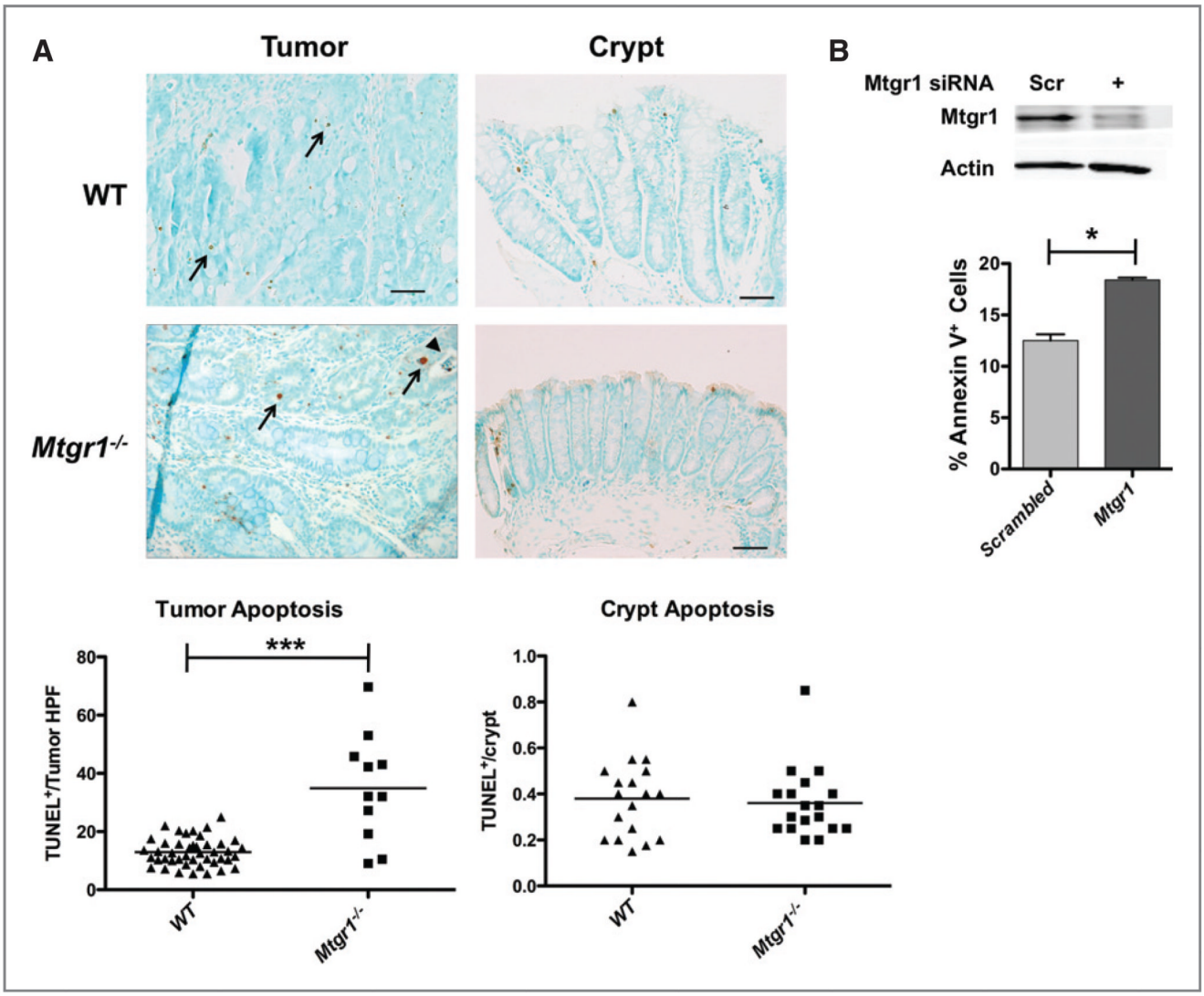

Figure 3.

Mtgr1$^{-/-}$ polyps demonstrate increased apoptosis. Colons were isolated from mice after completion of the AOM/DSS protocol. A, apoptosis was measured via TUNEL staining of Swiss rolled colons from all tumor bearing mice. *Mtrg1*$^{-/-}$ polyps, on average, have higher apoptotic cell counts than WT polyps (***$P < 0.001$) but there is no difference in apoptosis within crypts. B, siRNA knockdown of *Mtgr1* in the colon carcinoma line, HCT116, resulted in increased apoptosis compared to scrambled siRNA control (*$P < 0.05$). Error bar represents the standard deviation for three biological replicates.

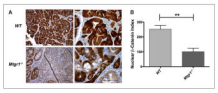

Figure 4.
Decreased expression and heterogeneous distribution of nuclear β-catenin in *Mtgr1*$^{-/-}$ tumors. β-catenin expression and localization was determined via immunohistochemistry with α-β-catenin as per Methods section. A, representative staining for β-catenin from WT or *Mtgr1*$^{-/-}$ tumors; B, β-catenin index (percentage of tumor with nuclear β-catenin × expression intensity (N = 10 mice, each genotype) $^{**}P < 0.01$). Error bar represents the standard deviation and scale bar is 5 μm.

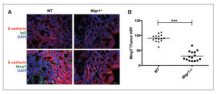

Figure 5.
Decreased expression and secretion of MMP7. A, immunofluorescence for MMP7 demonstrated a decrease in MMP7 production and secretion. E-cadherin, a downstream target of Mmp7 is shown in red. B, $MMP7^{+}$ cells were counted per 40× HPF in tumors from WT and $Mtgr1^{-/-}$ mice (***$P < 0.001$). Scale bar is 5 μm.

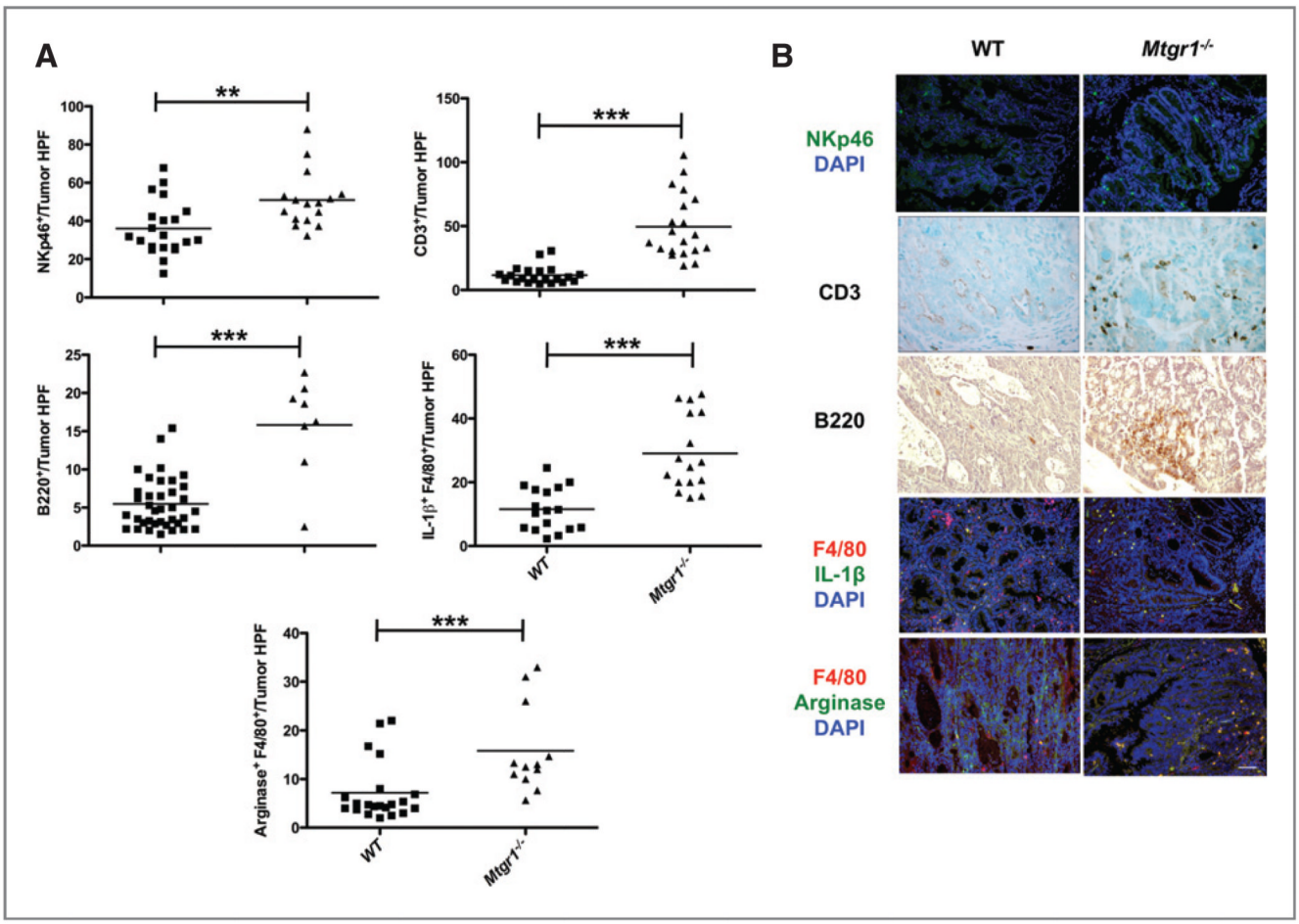

Figure 6.

Mtgr1$^{-/-}$ tumors have increased immune infiltration. A and B, WT or *Mtgr1*$^{-/-}$ tumors were stained with αNKp46 (green), αCD3, αB220, αF4/80 (red), αIL-1β (green), and αARG1 (green) antibodies and positive cells/tumor HPF were counted showing increased immune infiltrate in *Mtgr1*$^{-/-}$ tumors in comparison to WT tumors (***$P < 0.001$, **$P < 0.01$). Scale bar is 5 μm.

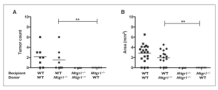

Figure 7.

Autologous transfer of *Mtgr1*$^{+/+}$ marrow does not reverse the *Mtgr1*$^{-/-}$ AOM/DSS phenotype. Bone marrow transplants were performed on WT and *Mtgr1*$^{-/-}$ mice as indicated. A, wild type mice given *Mtgr1*$^{-/-}$ bone marrow have more polyps per colon than *Mtgr1*$^{-/-}$ mice given WT bone marrow (**$P < 0.01$). B, colonic polyps are larger in WT mice rescued with *Mtgr1*$^{-/-}$ bone marrow than in *Mtgr1*$^{-/-}$ mice rescued with WT marrow.